Renewable Energy 95 (2016) 178–190

Contents lists available at ScienceDirect

Renewable Energy

journal homepage: www.elsevier.com/locate/renene

# Comparative analysis of the infield response of five types of photovoltaic modules

Ion Visa, Bogdan Burduhos**, Mircea Neagoe, Macedon Moldovan, Anca Duta*

*R&D Center: Renewable Energy Systems and Recycling, Transilvania University of Brasov, Romania*

ARTICLE INFO

*Article history:*
Received 31 December 2015
Received in revised form
2 March 2016
Accepted 1 April 2016
Available online 13 April 2016

*Keywords:*
Infield photovoltaic response
Photovoltaic output
Photovoltaic efficiency
BIPV

ABSTRACT

Five types of photovoltaic (PV) modules were comparatively analyzed considering the electrical output, efficiency and relative loss in efficiency, based on infield data collected in a temperate mountain climate, over 14 months. The mono-, poly-crystalline silicon, CdTe, CIS and CIGS modules were mounted on two identical platforms, installed close to a row of buildings. Based on the data collected from individual or groups of modules on the two platforms, analyses focused on the photovoltaic output, considering: the mean monthly values; the influence of the neighboring buildings; the influence of the irradiance, temperature and wind in different seasons (winter, summer); the influence of tracking on each PV module type. The qualitative analysis shows that small PV platforms installed in the built environment require accurate investigations on the air currents with influence on snow and frost retention/melting and water vapor condensation. In the temperate climate, with snowy winters and rather warm summers, the best performing modules are of poly-crystalline silicon; among thin film modules, the best output corresponds to CIGS, while the steadiest efficiency corresponds to CdTe. Tracking has a "leveling" effect on the conversion efficiency, making the PV output more predictable during days with preponderant direct solar irradiance.



## 1. Introduction

Extended research is devoted to estimate the photovoltaic infield conversion efficiency as a prerequisite for accurate design of feasible and affordable systems; literature outlines that the main factors affecting the conversion efficiency are: the PV type/materials, the amount of incident solar irradiance and the operating temperature [1,2]. These factors are further depending on specific features of the implementation location (geographical coordinates, climatic profile) and on parameters such as the ambient and PV module temperature variation with wind, etc.

The infield conversion efficiency is important in the output prediction for an adequate balance of system, BOS. Additionally, the correct estimation of the electricity production represents a bottleneck in the feasible exploitation of PV systems, as in several countries a 24 h advance is set for selling the next day PV production; any overproduction is not part of the trade, while any under-estimation is penalized. Therefore, prediction algorithms are developed and a recent analysis shows that there is no need for complex models if reliable calibration data are available [3].

The accurate knowledge on the photovoltaic response is time consuming, as reliable data are required for at least one full year of monitoring; therefore, there is a need for analyzing infield data of various PV module types, and outline novel findings/correlations for typical locations.

An important application of PV systems is the built environment. In the near future, new and existing buildings have to meet strict energy consumption standards in order to comply with the nZEB (Nearly Zero Energy Building) status, which implies that a building produces at least 50% of its energy demand using renewables installed on or nearby. Photovoltaics are main candidates, installed on suitably oriented roofs, rooftops, façades or individual arrays. Hereby, one constraint is related to the available area for PVs mounting, thus the system design requires accurate estimation of the infield efficiency, supporting the selection of best performing PV modules in the implementation location and the PV array dimensioning [4].

Literature addresses the variation in the conversion efficiency of different PV technologies implemented in the built environment

* Corresponding author.
** Corresponding author.
*E-mail addresses:* bogdan.burduhos@unitbv.ro (B. Burduhos), a.duta@unitbv.ro (A. Duta).

http://dx.doi.org/10.1016/j.renene.2016.04.003
0960-1481/

[5,6], but recommendations on the best PV module type(s) for a given climatic profile are scarce.

The analysis of different PV types using mathematical models can be used. Three PV types (mono-, poly-crystalline and amorphous silicon) were analyzed [7] covering the materials physics and the cost analysis; simulations based on meteorological data are reported [8], to define the behavior of four PV types: amorphous silicon (a-Si), tandem structure of amorphous silicon and microcrystalline silicon, CdTe and polycrystalline silicon (p-Si).

More accurate is the infield testing of different installed PV types; usually papers analyze no more than three PV types, as the comparative analysis of monocrystalline silicon (m-Si), p-Si and CdTe [9], or the study on p-Si, a-Si, and heterojunction with intrinsic thin layer (HIT), [10]. A comparative analysis of eight PV parks (with p-Si, a-Si, CdTe, GaAs or HIT modules) was recently reported concluding on the infield output and on the enhancement brought by tracking [11]. The PV modules reported in these papers are mainly serially connected, when a defect or lower-rated module will influence the result of the entire string. This solution also limits the possibility to compare modules of same type subjected to identical (PV mismatch) or different (shading) conditions [12].

Based on infield data collected over 14 months, this paper comparatively analyses the photovoltaic response of five PV module types (p-Si, m-Si, CIGS, CdTe and CIS); each module/group of modules has a power optimizer, further connected to an inverter. This setup allows to individually monitor the delivered power, thus the conversion efficiency and the relative losses. Two identical platforms are implemented in the built environment allowing comparison on the average output and on the deviations, correlated with specific features in the mountain temperate climate.

## 2. Experimental set-up

The experimental set-up is installed in a mountain temperate climate region (Brasov, Romania, 45.65°N, 25.65°E, 600 m above the sea level); the data were collected between July 2014 and August 2015.

A *Solys2* tracking system (Kipp & Zonen) measured the solar irradiance; it consists of a ball-shaded pyranometer for the diffuse solar irradiance (CMP22, ISO Secondary Standard, 1% daily uncertainty) and a pyrheliometer for the direct solar irradiance (CHP1, ISO First Class, 1% daily uncertainty). A *DeltaT* weather station measured the ambient temperature (RHT2 sensor, 0.1 °C accuracy), relative humidity (±2% accuracy), wind direction (WD1 wind vane, ±2° accuracy) and wind speed (AN1 anemometer, 1% accuracy). Sensors (PT100) are mounted on the back of each module for temperature monitoring.

Five different PV module types were used: p-Si and m-Si (noted as “poli” and, respectively “mono” in the graphs), and the thin film CIGS, CdTe and CIS; the parameters measured in standard testing conditions (STC) are given in Table 1. The thin-film modules were parallel connected, in groups of two (CIGS and, respectively CIS) or three modules (CdTe) to get a power similar to that of the silicon-based ones. The electrical output parameters of the photovoltaic modules are monitored for each module/group of modules using *Solaredge* components (a SE2200 single-phase inverter and P405 power-optimizers; accuracy of 2.5% in voltage and current). At least 7 power-optimizers are required to fit the nominal voltage of the invertor, therefore an array design was chosen consisting of 2 independent p-Si, 2 independent m-Si modules, 1 group of two parallel CIGS modules, 1 group of three parallel CdTe modules and 1 group of two parallel CIS modules, Table 1.

This array design (Fig. 1) was replicated on two identical platforms, P2 and P4, to test possible deviations in the output energy.

The platforms are part of a larger outdoor experimental set-up, Fig. 2, consisting of five platforms (P1 … P5), installed near the 12 laboratory buildings of the R&D Institute of the Transilvania University of Brasov. The P1, P3 and P5 platforms have only m-Si and p-Si modules.

The site has low wind potential with a predominant SE direction, with the strongest winds coming from W and NW, [13]. The laboratory buildings are developed as nZEB, with metallic coverage high insulating façades; the S-facing façades heat faster thus may generate air currents that can influence the PV output. These local currents are close to the ground and are not sensed by the anemometers on the weather station, thus are not part of the wind rose

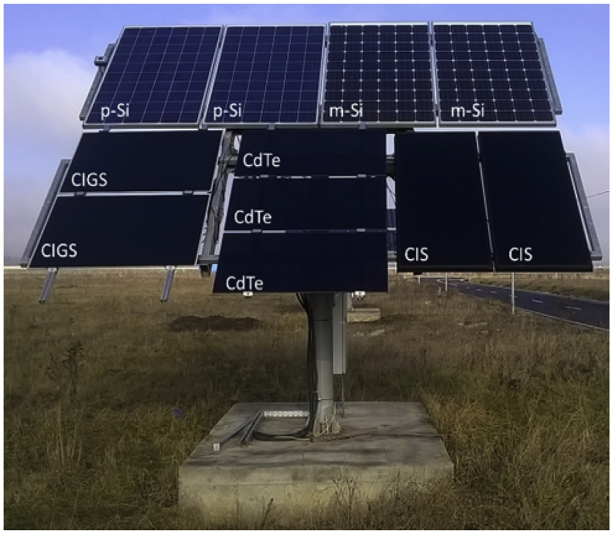


**Fig. 1.** Platform P2 with five types of PV modules.

**Table 1**
Standard testing conditions (STC) parameters of the five types of photovoltaic modules.

| | p-Si | m-Si | CIGS | CdTe | CIS |
|---|---|---|---|---|---|
| Manufacturer | LDK | Heliene | Solibro | Calyxo | Avancis |
| Product code | LDK-250P-20 | HEE215M | SL2-120 | CX3 80 | Powermax Strong 125 |
| Peak power $P_{max}$ [W] | 250 (±3%) | 250 (±3%) | 120 (+4%) | 80 (±5%) | 125 (+4%) |
| Maximum voltage Vm [V] | 30.2 | 30.8 | 76.9 | 47.0 | 43.8 |
| Maximum current Im [A] | 8.28 | 8.12 | 1.56 | 1.72 | 2.85 |
| Open circuit voltage Voc [V] | 37.5 | 37.4 | 97.6 | 62.8 | 59.1 |
| Short circuit current Isc [A] | 8.59 | 8.67 | 1.69 | 2.01 | 3.24 |
| Nominal Efficiency [%] | 17.12 | 17.94 | 13.54 | 11.89 | 13.04 |
| Photovoltaic area of a module [$m^2$] | 1.46 | 1.39 | 0.89 | 0.673 | 0.96 |
| STC temperature coefficient of $P_{max}$, Eq. (7) β [$°C^{-1}$] | 0.0045 | 0.0044 | 0.0038 | 0.0025 | 0.0039 |
| No. of modules in a group | 1 | 1 | 2 | 3 | 2 |
| No. of modules on a platform | 2 | 2 | 2 | 3 | 2 |

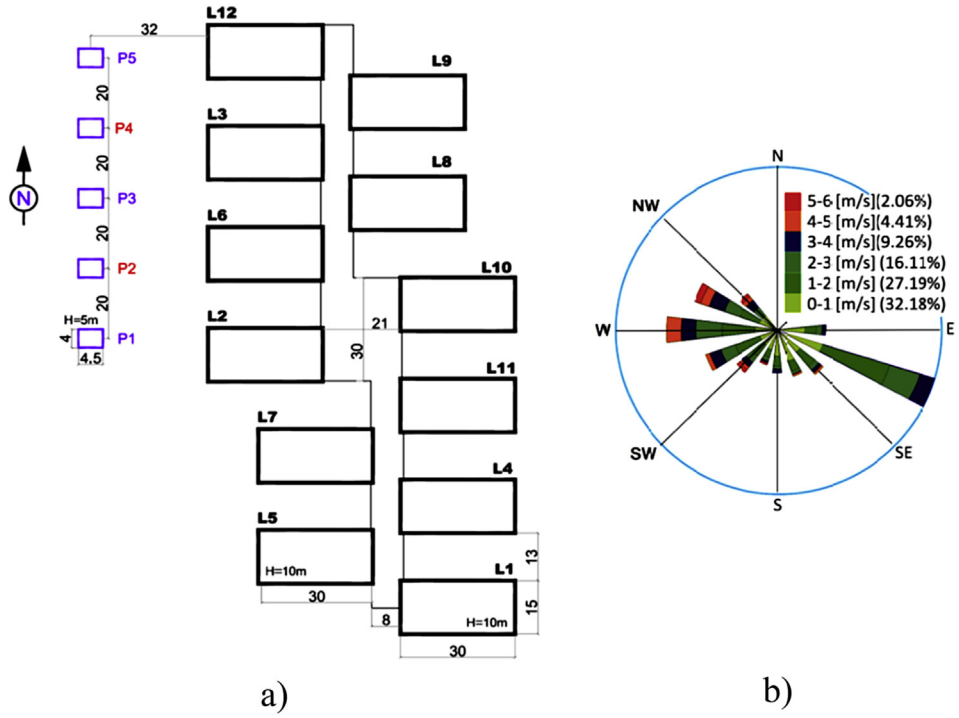


**Fig. 2.** a) The outdoor set-up with five PV platforms; b) the wind rose at the implementation location.

in Fig. 2b.

Both platforms are S – oriented, at a 47° tilt angle, selected based on infield observation, as recommended by other reports, [14]; the value is slightly higher than the latitude angle [15], and is the result of a climatic profile with snowy winters.

The platforms have dual-axis tracking systems and allow testing the tracking effect in the built environment, as presented in paragraph 3.4.

## 3. Results and discussions

The outdoor conversion efficiency, $\eta_{PV}$, was calculated based on infield data, Eq. (1):

$$\eta_{PV} = \frac{P}{G_{rec}A}\,100 \tag{1}$$

where: P is the output electrical power of a module/group of modules and $G_{rec}$ is the global solar irradiance received on a module/group of modules with the photovoltaic area, A.

The $G_{rec}$ value is the sum of the direct ($B_n$) and diffuse ($D_n$) radiation received by the photovoltaic area, calculated based on the direct irradiance (B) and the diffuse solar irradiance measured on the horizontal plane ($D_h$) given by the *Solys* station [13], as presented in Fig. 3 (where the ν, α and ψ angles depend on the day of the year, solar time and on the latitude of the implementation location, [16]).

By integrating $G_{rec}$ values for a preset time interval, the input solar energy, $E_{rec}$, can be calculated.

$$G_{rec} = Bn + Dn \tag{2}$$

$$B_n = B\cos\nu \tag{3}$$

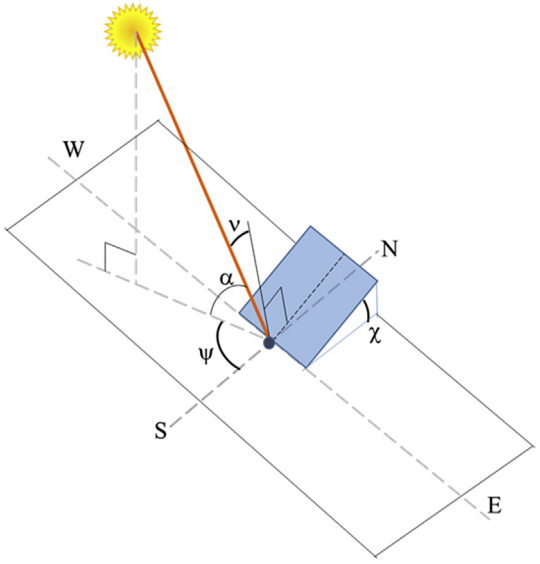


**Fig. 3.** Angles used in calculating $G_{rec}$.

$$\cos\nu = \cos\alpha\cdot\sin\chi\cdot\cos\psi + \sin\alpha\cdot\cos\chi \tag{4}$$

$$D_n = D_h(1+\cos\chi)/2 \tag{5}$$

ν: incidence angle of the sun ray on the photovoltaic surface;
α: solar altitude angle;
ψ: solar azimuth angle
χ: tilt angle of the module.

The angles are defined related to the horizontal plane of the

observer.

The relative loss in efficiency, $\Delta\eta_{PV,}$ previously formulated as a synthetic indicator of the PV modules infield performance [17], is defined by Eq. (6):

$$\Delta\eta_{PV} = \left[\left(\eta_{ref} - \eta_{PV}\right)\Big/\eta_{ref}\right]*100 \quad (6)$$

where: $\eta_{PV}$ represents the outdoor conversion efficiency and $\eta_{ref}$ is the nominal efficiency.

### 3.1. Annual variation of the photovoltaic output

The annual variation of the output parameters (electric energy, infield efficiency and relative loss of efficiency) was estimated using monthly mean values, correlated with the input solar energy, $E_{rec}$. The results in Fig. 4a and b indicate that the electrical energy matches the solar input, with large amounts produced during summer months and a much lower winter production. The variation in the conversion efficiencies (Fig. 4c) indicates high values for the m-Si and p-Si modules and lower efficiencies of thin-film modules; however, these data outline larger monthly variations in the efficiency of the silicon-based modules and significantly lower variations throughout the year for the thin film modules, with more constant values for CdTe. These results might be the consequence of the thickness of the wafer cells which better supports heat storage that influences the conversion efficiency.

Temperature influences the photovoltaic output and is described by most manufacturers as Eq. (7), that models the efficiency at a cell/module working temperature, $T$, ($\eta_{PV,m}$) based on the efficiency $\eta_0$, measured at a reference temperature, $T_0$. Usually, the standard testing temperature (25 °C) is set as reference.

$$\eta_{PV,m} = \eta_0\,[1 - \beta(T - T_0)] \quad (7)$$

The infield results in Fig. 4c are in line with the STC temperature coefficients (β in Table 1) with significantly higher values corresponding to the m-Si and p-Si, as compared CdTe, CIS and CIGS.

The relative losses in efficiency in Fig. 4d show that, although the efficiency of all three thin-film modules was relative constant, only CIGS performs close to the nominal value, while CdTe and CIS have relative losses higher than 15%. The silicon-based modules show small losses (5 … 10%), thus their energy production can be better estimated if solar irradiance is well predicted. The highest relative losses correspond to the winter months (December and January) which could be surprising considering the outdoor temperatures that supports module temperatures close to reference or lower; however, these losses are mainly due to the snow, frost and ice that cover the modules, obstructing the access of the solar irradiance or reflecting it (as sub-heading 3.3. will discuss).

### 3.2. Site-dependent variation in the photovoltaic efficiency

One important issue in the accurate PV system design is the reproducibility of the photovoltaic response for a given module type, according to its implementation site in the built environment. Modules of same type installed on a platform had a similar behavior. However, the modules of same type installed on platform P2 and, respectively on P4 show rather different results, as Fig. 5 shows. Differences occur during the winter months (December 2014–February 2015), mainly as result of the snow that melts faster on platform P4 than on P2; snow differently lasted on the modules as result of a slightly different profile of the air currents around the buildings: platform P4 is positioned in an area where the buildings are blocking almost all the E, N-E and S-E winds, allowing the modules to get a higher temperature.

The average absolute deviation (AAD) in Table 2 indicates efficiency fluctuations between the modules/group of modules of same type installed on the P2 and, respectively on the P4 platforms; the monthly conversion efficiencies are denominated as $\eta_{PV,2}$ and $\eta_{PV,4}$ and AAD is calculated based on the correspondent values for each month (a total number of months NM = 14), using Eq. (8):

$$AAD = \frac{1}{NM}\sum_{1}^{NM}\left|\frac{\eta_{PV,2} - \eta_{PV,4}}{\eta_{PV,2}}\right|*100 \quad (8)$$

The differences between two modules of the same type are rather small considering the entire period of 14 months; however, one should be aware of far larger differences in the monthly values, with deviations of 5 … 10% (last column in Table 2). For the winter months these deviation can be related to snow retention, but the large differences in September (for the p-Si and CdTe modules) may originate from another side effect: water vapor condensation (from the morning humidity) on the PV modules surface, forming a thin water film that distorts the solar radiation; drying this film differently lasts on the two platforms, due to slightly different air currents circulation.

### 3.3. Influence of the climatic parameters on the photovoltaic output

To outline the specifics that influence the photovoltaic conversion in the built environment, two months with different climatic profile (January 2015 and August 2014) were selected. All the infield data further discussed are calculated as mean values of the values registered on platforms P2 and P4.

#### 3.3.1. Winter season (January 2015)

As the data in Fig. 6 show, the effect of the snow layer on the PV modules can be easily noticed during January 1 … 6 and in January 15, 2015 when the electricity production is almost zero for all modules; this is also evident when comparing to similar irradiance-temperature conditions (January 23 … 28, 2015) but with no snow on the modules, when the energy production, although small, is proportional to the input irradiance; huge relative efficiency losses (close to 100%) confirm this dysfunctional situation.

The snow effect extends for m-Si and p-Si modules also on January 7 and 8, as a possible consequence of the much rougher glass surface on these modules, which supports snow sticking if the ambient temperature is low enough (the ambient temperature was below −10 °C). This assumption is confirmed by the snow that fully covers the silicon PVs on platforms P3 and P5, in Fig. 7.

The influence of low temperatures ($T_{max} = -5$ … 12 °C) on the conversion efficiency is evident for all days with $E_{rec} > 1$ kW h/m$^2$ if the modules are not covered with snow/ice (second half of the month), when all conversion efficiencies (except CdTe) are above the nominal ones.

The data in Fig. 6 show that January 29 has high solar irradiance and temperatures allowing ice/snow melting, thus supports high output and low relative efficiency losses. However, even in such a day it is important to outline the variations in the energy production and efficiency, allowing BOS accurate management. The data in Fig. 8 show a very stable efficiency for all module types during the interval when the input irradiance has a smooth, continuous variation (10:48 … 15:36). However, radiation fluctuations show a fast response in efficiency variation (Fig. 8d), leading to fluctuating energy production (Fig. 8c).

The temperature on the PVs follows a similar trend for all the modules but significant variations are registered among different types: a similar heat storage effect is observed for the p-Si, m-Si and CIS modules, and lower temperatures are registered on the CdTe modules (Fig. 8b); despite this, the CdTe modules show the highest

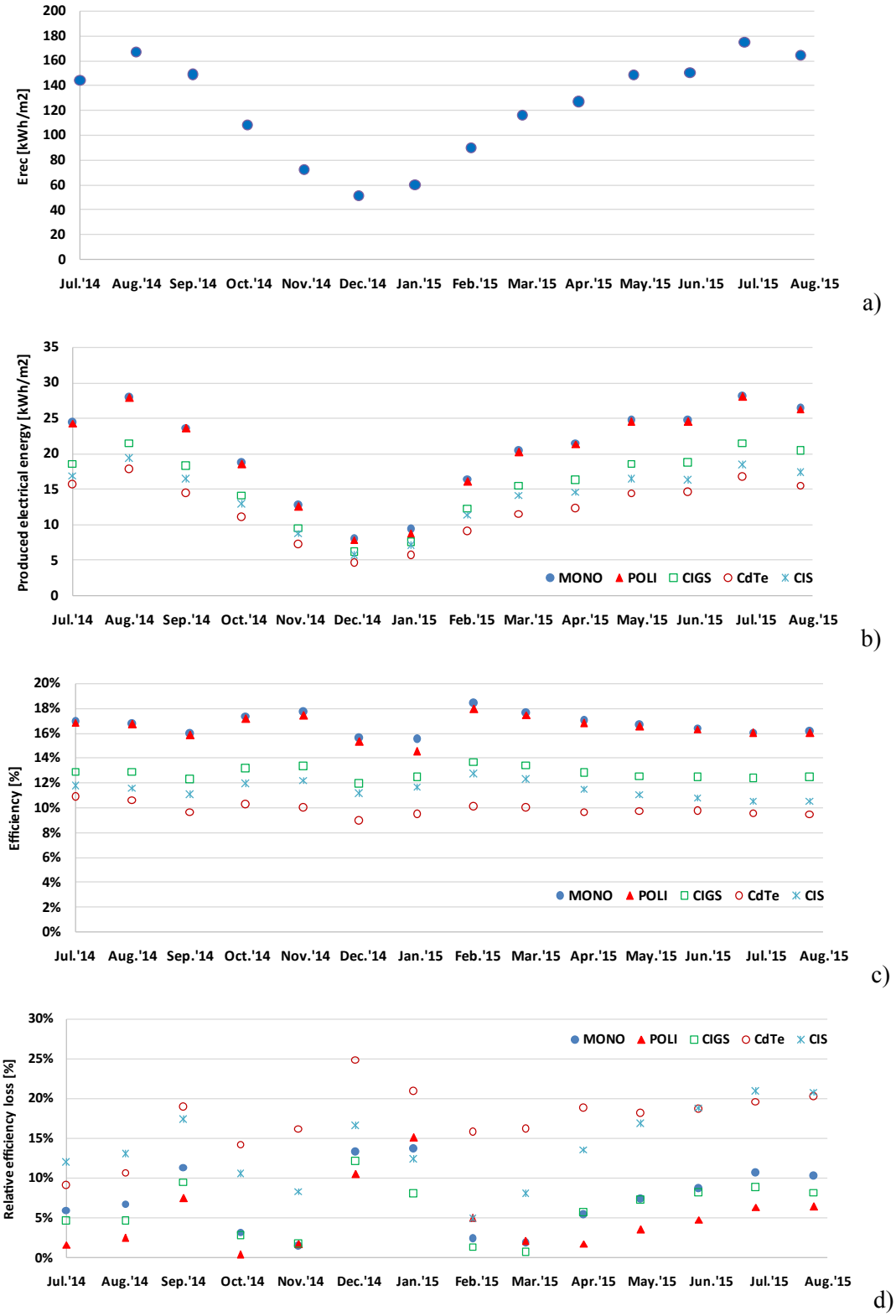


**Fig. 4.** Monthly variation of the: a) input solar energy; b) output electrical energy; c) outdoor conversion efficiency; d) relative efficiency loss (July 2014–August 2015).

relative efficiency loss, Fig. 8e, confirming other reports, [18].

The negative relative efficiency losses imply higher efficiencies than nominal. By applying Eq. (7) on a temperature interval of 0 …. 30 °C (measured on the modules) the data in Fig. 8f are obtained; the modelled efficiencies are lower compared to the infield ones, at low irradiance values (400 … 500 W/m$^2$), as result of the temperature coefficients which may have values depending on the irradiation amount, in good agreement with literature reports [19,20], outlining that diffuse radiation may support negative β values.

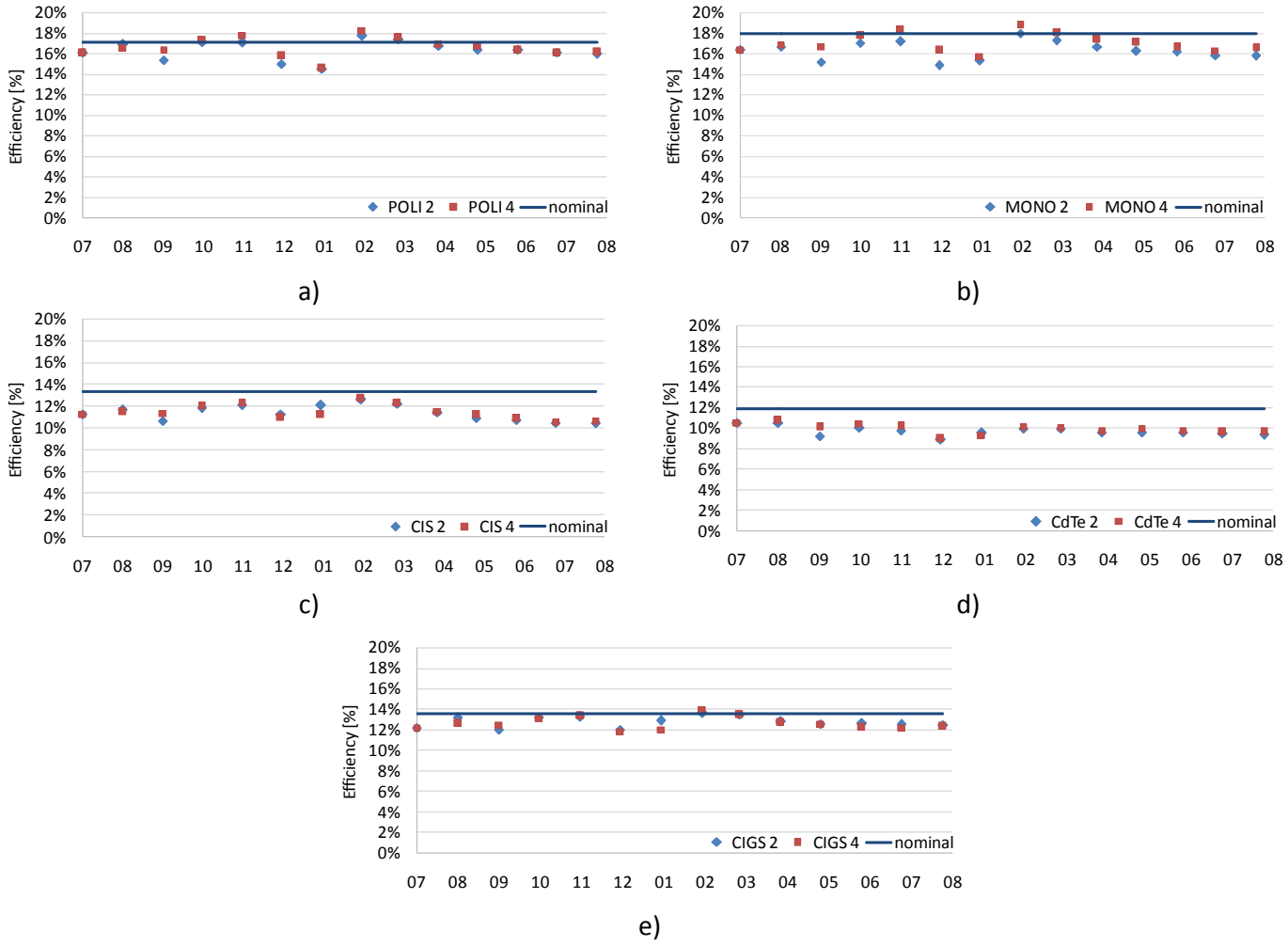


**Fig. 5.** Monthly average conversion efficiency of the PV modules/groups installed on platforms P2 and P4, compared with the nominal efficiencies: (a) p-Si; (b) m-Si; (c) CIGS; (d) CdTe; (e) CIS (July 2014–August 2015).

**Table 2**
Overall photovoltaic conversion data of the modules installed on P2 and P4.

| PV type | Overall production [kWh/m$^2$] | | Average efficiency $\eta_{PV}$ [%] | | Average absolute deviation, AAD [%] | Maximum monthly deviation P2 *vs.* P4 [%] | |
|---|---|---|---|---|---|---|---|
| | P2 | P4 | P2 | P4 | P2 *vs.* P4 | Month | Value |
| p-Si | 283.3 | 284.7 | 16.49 | 16.57 | 2.26 | September 2014 | 6.7 |
| m-Si | 281.3 | 291.5 | 16.37 | 16.97 | 2.33 | December 2014 | 5.1 |
| CIGS | 220.5 | 216.3 | 12.84 | 12.59 | 2.63 | January 2015 | 6.8 |
| CdTe | 167.9 | 171.8 | 9.78 | 10.00 | 3.30 | September 2014 | 10.3 |
| CIS | 194.6 | 195.4 | 11.33 | 11.37 | 2.69 | January 2015 | 7.1 |

### 3.3.2. *Summer season (August 2014)*

Following the same steps, August 2014 was investigated as a typical summer month. The data in Fig. 9 show similar output features for days with similar climatic profile.

Considering these results, four types of days could be outlined, considering the combination of solar irradiance and ambient temperature, Table 3. The data show that for a mountain climatic profile, with high, but not exceedingly high temperatures the most important factor governing the photovoltaic conversion is related to the amount and quality of solar radiation (direct *vs.* diffuse irradiance), as high amounts of solar energy on the module are responsible for larger energy losses. Oppositely, cloudy days (Type 1 and 2) allow slightly higher outdoor efficiencies than the nominal ones, for the m-Si and p-Si modules and low relative efficiency losses for the thin film modules.

The data confirm the cooling effect of the wind, as for days with high solar energy input, high ambient temperatures and higher wind speed (Type 3) significantly lower losses are registered, compared to the days with similar irradiance but with lower wind (Type 4), Fig. 9d. This effect can be enhanced by the built environment: there is a significant temperature difference between the S and the W – oriented façades (10 °C or above) in the experimental set-up, that can promote additional air currents.

This pattern can be extended to the cold months (e.g. January

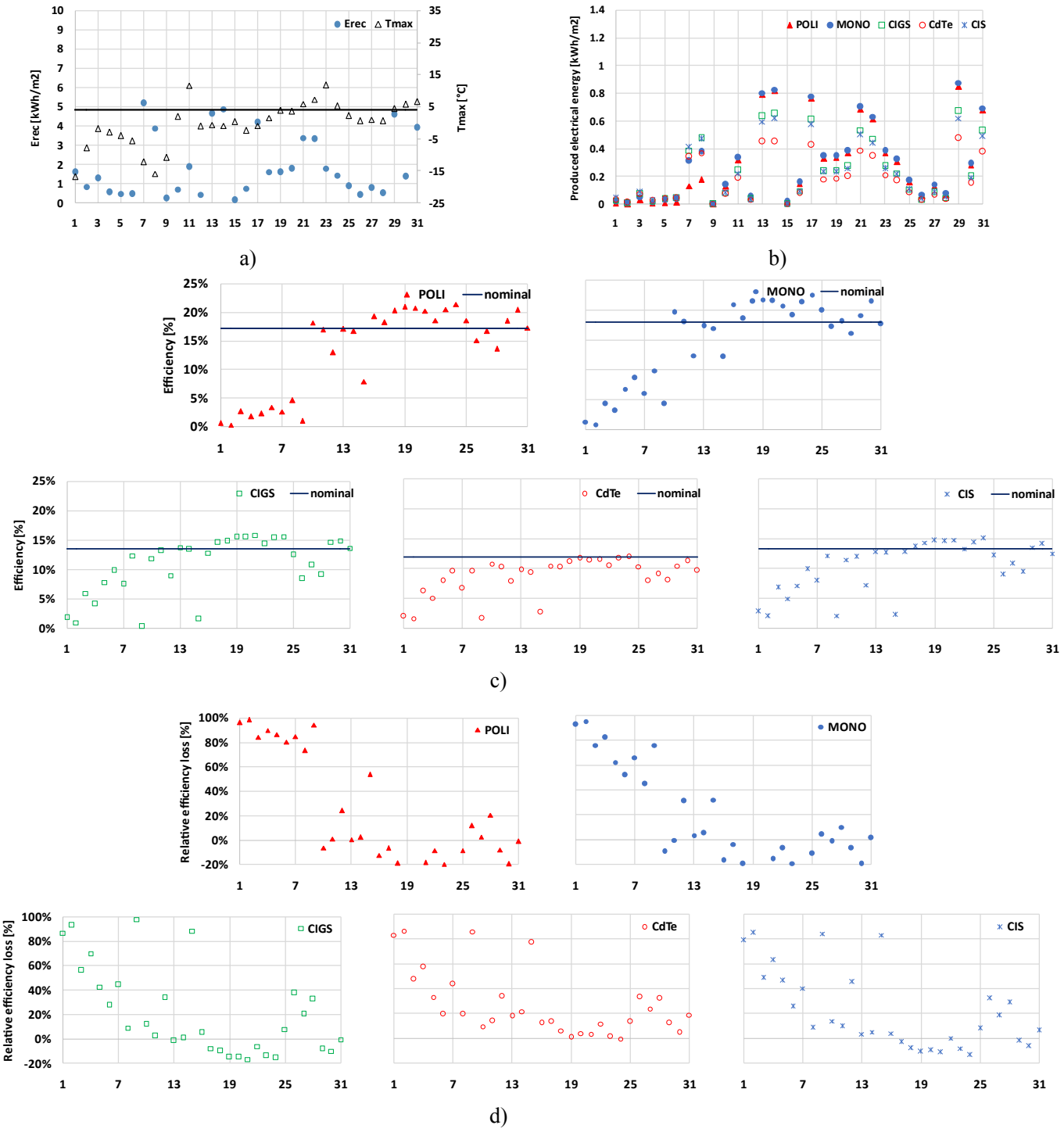


**Fig. 6.** Daily variation in a winter month of the: a) incident solar energy and ambient temperature; b) electrical energy output; c) conversion efficiency; d) relative efficiency loss (January 2015).

2015) when, during days without snow on the modules and with low temperatures (common in winter), the order in the relative efficiency loss is CdTe > CIS > CIGS = m-Si > p-Si, resembling the Type 4 days (the relative efficiency losses are different, with an obvious advantage during winter). Although not highly accurate, this approach could offer a tool to fast estimate the electrical energy production for the coming day, if the weather forecast is known.

One day with high energy production (August 1st, 2014, Fig. 10) was detailed analyzed. This is an almost complete sunny day, with a small irradiance fluctuation at the end of the day (16:00 … 17:00). The continuous variation and high values of the available ($G_{available}$) and of the incident irradiance on the modules ($G_{rec}$) indicates beam radiation as main input component. The output electrical power well follows the irradiance curves, Fig. 10b; despite this fact, during midday, at high incident solar irradiance and PV module temperatures, the conversion efficiency has the lowest values for all


**Fig. 7.** Different snow cover of the infield PV modules.

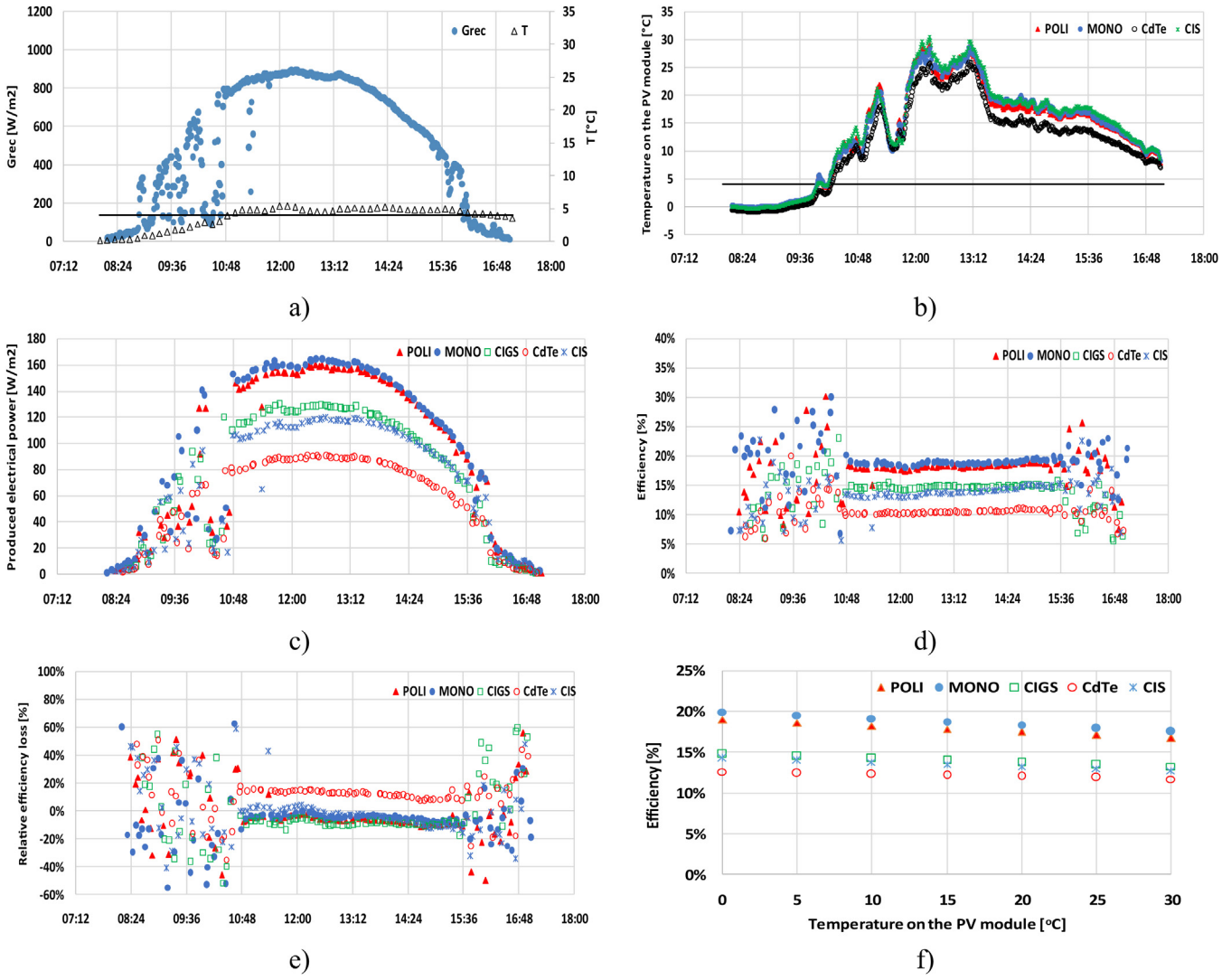


**Fig. 8.** Instantaneous variation of the: a) incident solar irradiance and ambient temperature; b) PV modules temperature; c) photovoltaic power output; d) conversion efficiency; e) relative efficiency loss; f) modelled efficiency at different temperatures (29 January 2015).

module types, Fig. 10c and d.

The insets in Fig. 10a and c focus on a sudden increase in the conversion efficiency during the fluctuating incident solar irradiance (most probably, a passing cloud); this may be explained by the thermal inertia of the PV modules or by the minute-sized delays between the irradiance and the electrical power measurements. To avoid such possible artefacts, a mediated hourly analysis is recommended.

This approach was further used for a day combining sunny and cloudy periods, August 22nd, 2014, and the results are presented in Fig. 11.

The fluctuating global (and direct) irradiance is representative for all days when high conversion efficiencies were registered, as result of lower temperatures on the PV modules (lower ambient

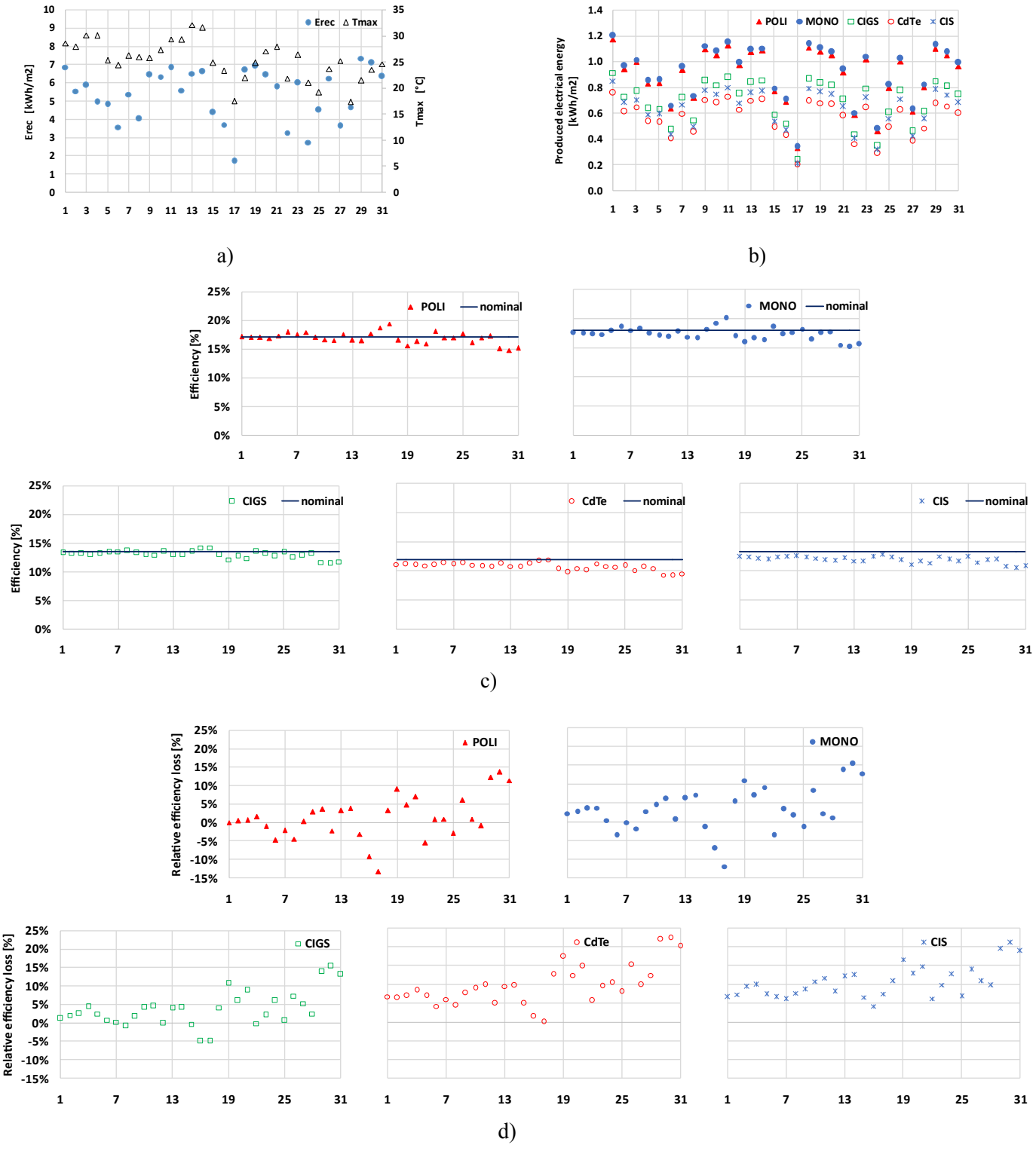


**Fig. 9.** Daily variation in a summer month of the: a) incident solar energy and ambient temperature; b) electrical energy output; c) conversion efficiency; d) relative efficiency loss (August 2014).

temperatures and lower direct heating). The electrical output, Fig. 11b, is low but follows the irradiance profile.

The data in Fig. 11c show that the hourly conversion efficiency of m-Si and p-Si modules varies almost linearly throughout the day, with very small, even negative relative efficiency losses during intervals with preponderant diffuse irradiance (~300 W/m$^2$), confirming the effect of diffuse radiation on the thermal coefficient of Si-based modules, [20]. Oppositely, the conversion efficiency of thin-film modules very much depends on the incident global solar irradiance and values of the solar input lower than 100 W/m$^2$ are insignificantly converted by these modules (e.g. the time interval after 18:00). As Fig. 11d outlines, CIS shows the worst response to

**Table 3**
Generic types of days with similar features of the photovoltaic conversion in August 2014.

| Day type | Irradiance | Ambient temperature | Wind speed | Relevant days in August 2014 | Relative efficiency losses |
|---|---|---|---|---|---|
| Type 1 | $E_{rec}$ < 5 kW h/m$^2$ (preponderant diffuse radiation) | Low T < 25 °C | 1.5 … 2 m/s | 15, 16, 17, 22 | CIS (7%) > CdTe (0%) > CIGS (−5%) > m-Si (−12%)) > p-Si (−14%) |
| Type 2 | $E_{rec}$ < 5 kW h/m$^2$ (preponderant diffuse radiation) | Average T = 25 … 27 °C | 1 m/s (morning) …. 5 m/s (noon, afternoon) | 6, 8, 27 | CIS (7%) > CdTe (4%) > CIGS (1%) > m-Si (−4%) > p-Si (−5%) |
| Type 3 | $E_{rec}$ > 5 kW h/m$^2$ (preponderant direct radiation) | High T > 27 °C | Max. 4 m/s | 1, 13, 14 | CIS (12%) > CdTe (10%) > m-Si (7%) > CIGS (5%) > p-Si (4%) |
| Type 4 | $E_{rec}$ > 5 kW h/m$^2$ (preponderant direct radiation) | Average T = 25 … 27 °C | Max. 1 m/s | 19, 29, 30, 31 | CdTe (23%) > CIS (22%) > m-Si = CIGS (16%) > p-Si (13%) |

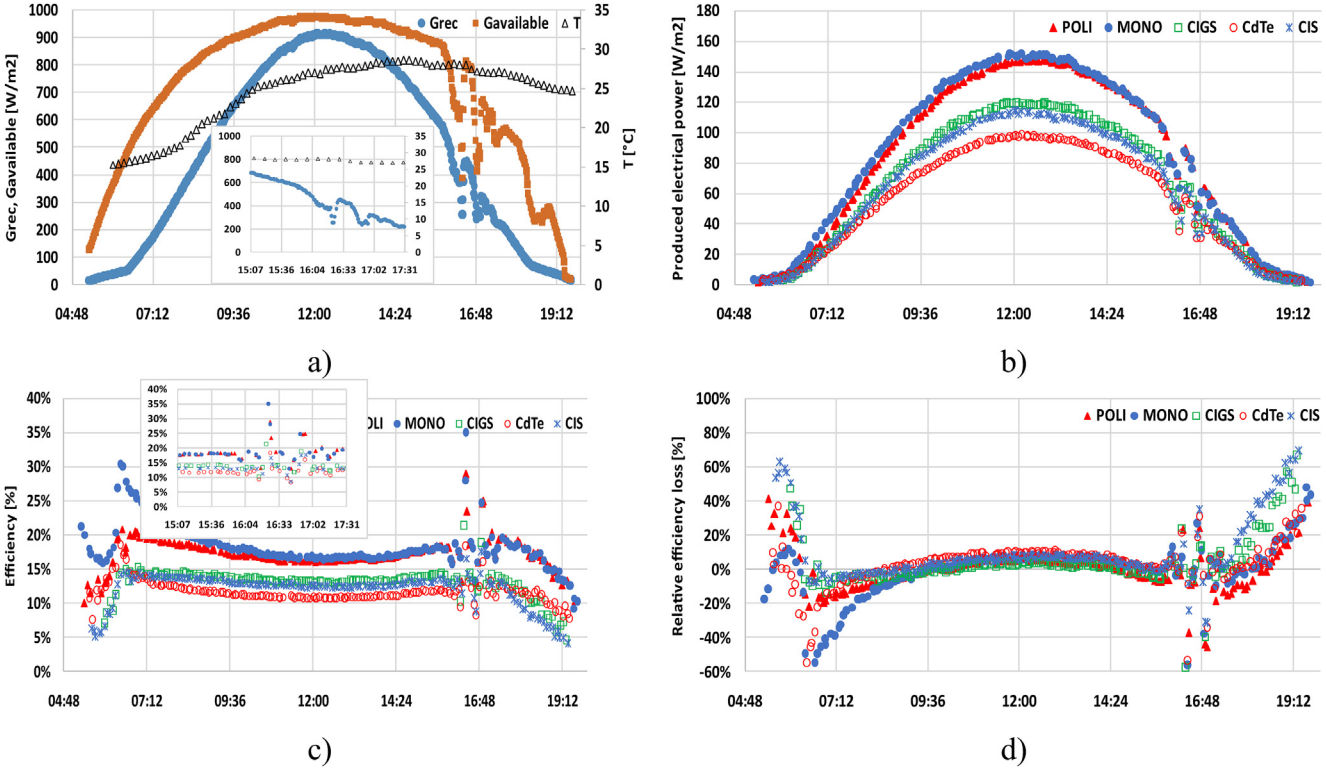


**Fig. 10.** Instantaneous variation during 1 August 2014 (day with highest energy production) of the: a) incident/available solar irradiance and ambient temperature; b) photovoltaic power output; c) conversion efficiency; d) relative efficiency loss.

low irradiance and CIGS has the largest variation in efficiency, making difficult to accurately predict the daily output.

This sensitivity to the solar irradiation amount may recommend tracking as a solution to increase the output and to get steadier efficiencies.

### 3.4. PV modules tracking the sun

Tracking enhances the PV output, but the combination of irradiance, temperature and wind will govern the amount of energy gain, [21]. According to the results in Fig. 11, the modules (mainly the thin film ones) are converting solar energy only at irradiance values higher than 100 … 200 W/m$^2$. Thus the tracking algorithm should be limited to the modelled solar time corresponding to irradiance values higher than 200 W/m$^2$.

A day combining high irradiance and average temperature was selected, (September 19, 2015; Type 4 day), to discuss the tracking effect(s); the tracking algorithm was implemented during the time interval with irradiance higher than the stated threshold. Comparing to the data in Fig. 10 (also corresponding to a sunny day), the results in Fig. 12 show an increase in the power output of all tracked modules on the P2 platform.

As the data in Fig. 12 show, tracking increases the steadiness of the conversion efficiency values, making the PV systems more predictable. This effect is distorted in some extent by the temperature increase on the modules, thus the average relative losses in efficiency follow the order: CIS = CdTe (38%) > m-Si (22%) > p-Si (19%) > CIGS (16%). This drawback explains why the output power is only with 10% higher as compared to the output obtained on the fixed platform (P4).

During days with preponderant diffuse irradiance as 31.07.2015, when the ratio diffuse/global irradiance exceeds 0.9, the output of tracked and non-tracked modules is almost the same, and tracking is not justified, Fig. 13. However, the leveling effect of tracking on the conversion efficiency is preserved if irradiance is higher than the threshold value.

These types of studies will be extended in the future by correlating the photovoltaic output with solar radiation models that

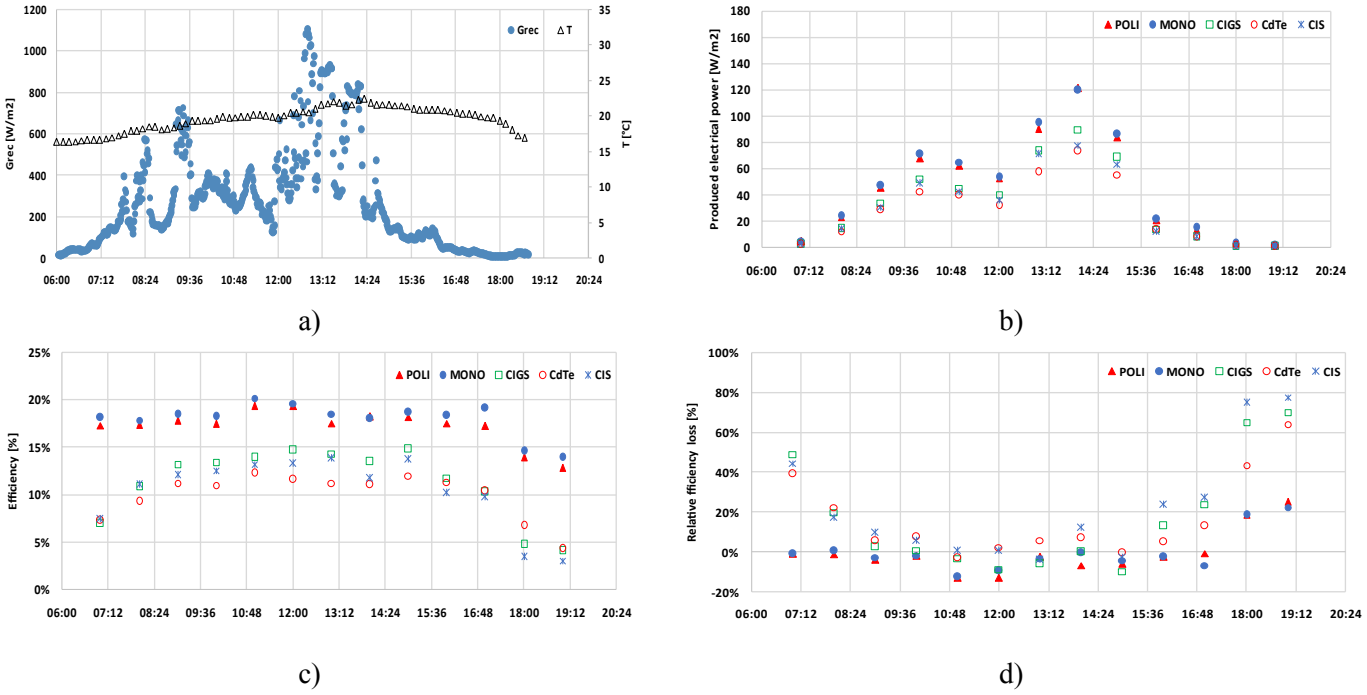


**Fig. 11.** Variation of the: a) instantaneous incident solar irradiance and ambient temperature; b) photovoltaic power output; c) conversion efficiency; d) relative efficiency loss (22 August 2014).

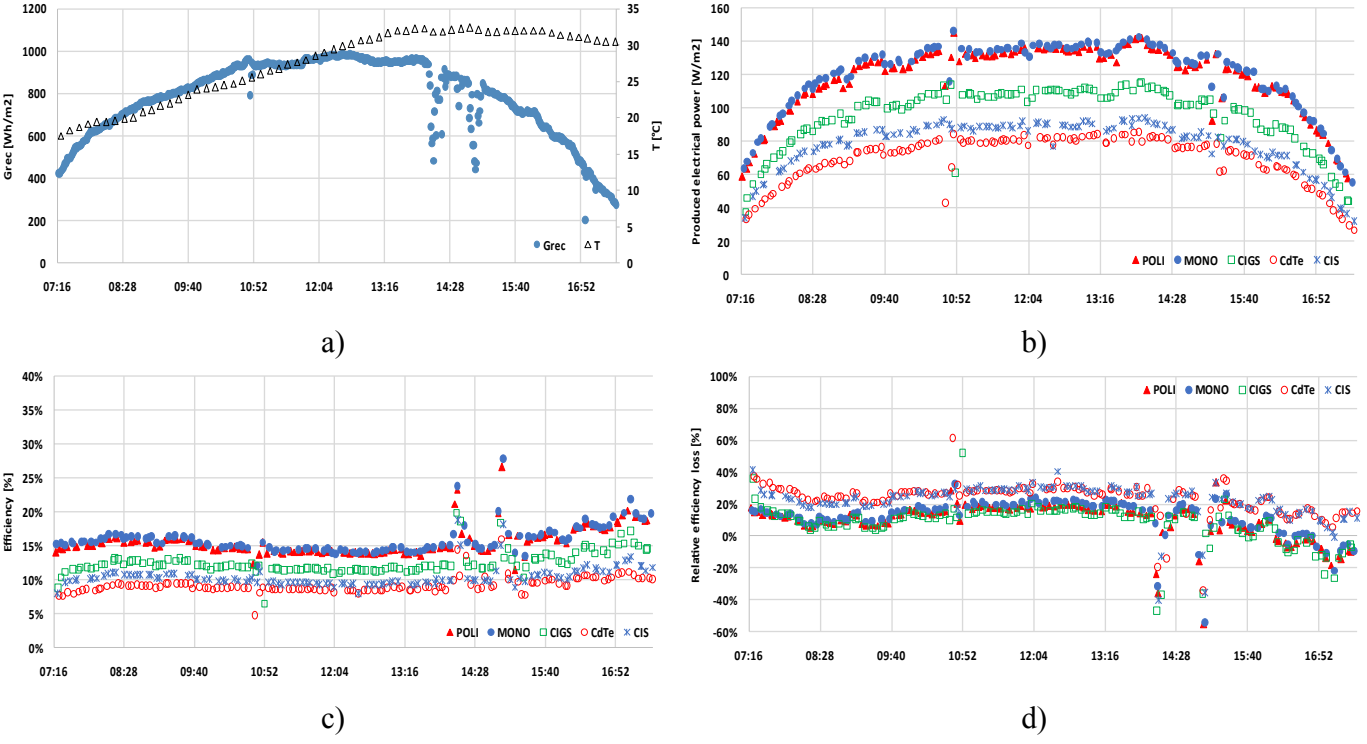


**Fig. 12.** Instantaneous variation of: a) incident solar irradiance and ambient temperature; b) photovoltaic power output; c) conversion efficiency; d) relative efficiency loss (September 19, 2015).

should be able to replace the infield data; satellite solar radiation models [22], or algorithms based on sky camera images [23], could be employed for an accurate prediction.

## 4. Conclusions

A comparative analysis of five different PV modules types (m-Si, p-Si, CIS, CIGS and CdTe) outlines that there are local factors that significantly influence the PV output in the built environment, as

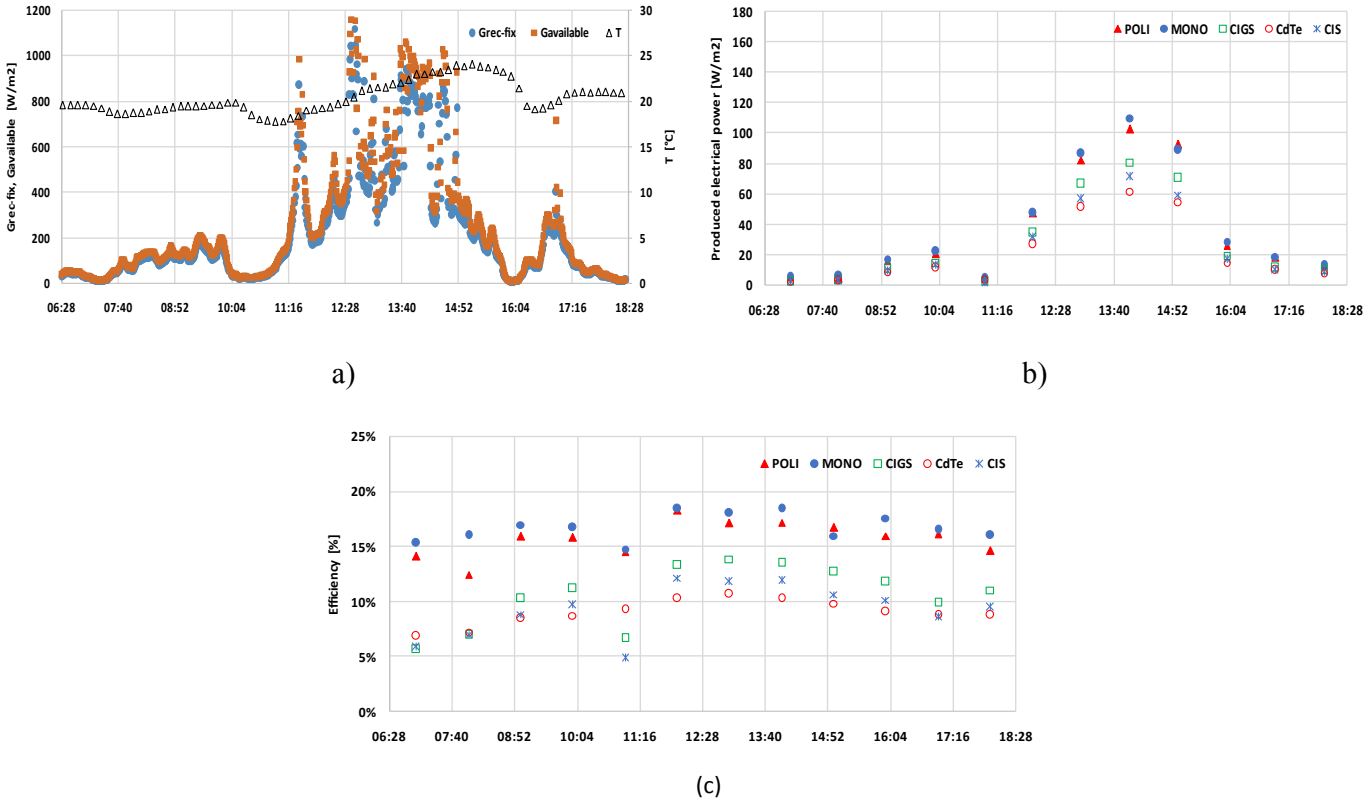


**Fig. 13.** Instantaneous variation of the: a) solar irradiance and ambient temperature; b) photovoltaic power output; (c) conversion efficiency (31 July 2015).

snow, frost, condensed water vapors; their effect is enhanced by the air currents circulation that supports lower or higher onsite temperatures.

The photovoltaic output, the efficiency and the relative loss in efficiency were analyzed; the results show that in a mountain temperate climate, with cold, snowy winters and with sunny summers the best performing modules are p-Si, m-Si and CIGS, while high relative efficiency losses are observed for the CIS and CdTe thin film modules.

The transparent glass surface on the PV modules plays a significant role during winter; rough surfaces can increase the snow retention on the modules, blocking the irradiance access, as it was found for the m-Si and p-Si modules. The snow will melt even slower if the modules are implemented in windy places or in locations with more active air circulation. Thus, a PV array should be implemented in the built environment after developing a wind chart of the implementation site, measured at the height of the PV array.

The combination of input solar irradiance, ambient temperature and wind speed allowed to qualitatively define four generic types of days, each being characterized by similar trends in the output indicators. Based on a one year (or more) monitoring, the PV output during these 4 types of days can be estimated for each month, allowing to predict the photovoltaic production in a given location.

The paper shows that tracking has a leveling effect on the conversion efficiency, during days with predominant direct irradiance. A high and almost similar power output for the p-Si and m-Si modules was found, while the lowest values were registered for the CdTe modules. However, the CdTe modules show the steadiest conversion efficiencies, both in the tracked and tilt fixed modes.

This type of analysis is recommended before selecting the PV modules to be installed in the built environment or in large facilities (as PV parks). For the temperate continental climate with snowy winters, the results show that p-Si modules are well suited if rough glazed PV surfaces are avoided. On the other hand, in a cost-benefit analysis, the thin films modules can be competitive if the available implementation surface is not a limiting condition, and the CIGS module are recommended for the typical climatic profile analyzed in this paper. In a broader approach, the results show that there is a need for improving the models describing the photovoltaic conversion, by further adding the influence of various climatic parameters as moisture (air humidity), frost or snow likelihood, etc.

## Acknowledgement

This work was done in the frame of the project EMAX-BIPV, PN-II-RU-TE-2014-4-1763, contract no. 131/1.10.2015, financed by the Romanian National Research Council (ANCS, CNDI-UEFISCDI), within the Romanian Research Program: Human Resources - Research Projects for Young Research Teams, RU-TE-2014 Subprogram.

## References

[1] M.C. Di Vincenzo, D. Infield, Detailed PV array model for non-uniform irradiance and its validation against experimental data, Sol. Energy 97 (2013) 314–331.
[2] W. Teixeira da Costa, J. Farias Fardin, L. de Vilhena, B. Machado Neto, Domingos Sávio Lyrio Simonetti, Estimation of irradiance and temperature using photovoltaic modules, Sol. Energy 110 (2014) 132–138.
[3] A. Dolara, S. Leva, G. Manzolini, Comparison of different physical models for PV power output prediction, Sol. Energy 119 (2015) 83–99.
[4] G. Cattarin, F. Causone, A. Kindinis, L. Pagliano, Outdoor test cells for building envelope experimental characterisation – a literature review, Renew. Sustain. Energy Rev. 54 (2016) 606–625.
[5] L. Mature, G. Belluardo, D. Moser, M. Del Buono, BiPV system performance and

efficiency drops: overview on PV module temperature conditions of different module types, Energy Procedia 48 (2014) p.1311–1319.
[6] A.J. Carra, T.L. Pryorb, A comparison of the performance of different PV module types in temperate climates, Sol. Energy 76 (1–3) (2004) 285–294.
[7] S. Yilmaza, H.R. Ozcalika, S. Keslerb, F. Dincerc, B. Yelmend, The analysis of different PV power systems for the determination of optimal PV panels and system installation—a case study in Kahramanmaras, Turkey, Renew. Sustain. Energy Rev. 52 (2015) 1015–1024.
[8] C. Cañete, J. Carretero, M. Sidrach-de-Cardona, Energy performance of different photovoltaic module technologies under outdoor conditions, Energy 65 (2014) 295–302.
[9] M.E. Başoğlu, A. Kazdaloğlu, T. Erfidan, M.Z. Bilgin, B. Çakır, Performance analyzes of different photovoltaic module technologies under İzmit, Kocaeli climatic conditions, Renew. Sustain. Energy Rev. 52 (2015) 357–365.
[10] V. Sharma, A. Kumarb, O.S. Sastryb, S.S. Chandela, Performance assessment of different solar photovoltaic technologies under similar outdoor conditions, Energy 58 (1) (2013) 511–518.
[11] A. Bianchini, M. Gambuti, M. Pellegrini, C. Saccani, Performance analysis and economic assessment of different photovoltaic technologies based on experimental measurements, Renew. Energy 85 (2016) p.1–11.
[12] J. Bai, Y. Cao, Y. Hao, Z. Zhang, S. Liu, F. Cao, Characteristic output of PV systems under partial shading or mismatch conditions, Sol. Energy 112 (2015) 41–54.
[13] I. Visa, C. Jaliu, A. Duta, M. Neagoe, M. Comsit, M. Moldovan, D. Ciobanu, B. Burduhos, R. Saulescu, The Role of Mechanisms in Sustainable Energy Systems, Transilvania University Press, Brasov, 2015, p. 49. ISBN 978-606-19-0571-3.
[14] A.K. Yadav, S.S. Chandel, Tilt angle optimization to maximize incident solar radiation: a review, Renew. Sustain. Energy Rev. 23 (2013) 503–513.
[15] C.L. Cheng, S. Charles, S. Jimenez, M.-C. Lee, Research of BIPV optimal tilted angle, use of latitude concept for south orientated plans, Renew. Energy 34 (6) (2009) 1644–1650.
[16] S. Kalogirou, Solar Energy Engineering. Processes and Systems, second ed., Academic Press, 2014.
[17] I. Visa, M. Comsit, M.D. Moldovan, A. Duta, Outdoor simultaneous testing of four types of photovoltaic tracked modules, J. Renew. Sustain. Energy 6 (3) (2014). Article Number: 033142.
[18] A. Carullo, F. Ferraris, A. Vallan, F. Spertino, F. Attivissimo, Uncertainty analysis of degradation parameters estimated in long-term monitoring of photovoltaic plants, Measurement 55 (2014) 641–649.
[19] E. Skoplaki, J.A. Palyvos, On the temperature dependence of photovoltaic module electrical performance: a review of efficiency/power correlations, Sol. Energy 83 (5) (2009) 614–624.
[20] C.M. Whitaker, T.U. Townsend, H.J. Wenger, A. Iliceto, G. Chimento, F. Paletta, Effects of irradiance and other factors on PV temperature coefficients, in: Photovoltaic Specialists Conference, 1991, Conference Record of the Twenty Second IEEE, 1, 1991, pp. 608–613.
[21] S.A. Sharaf Eldin, M.S. Abd-Elhady, H.A. Kandil, Feasibility of solar tracking systems for PV panels in hot and cold regions, Renew. Energy 85 (2016) 228–233.
[22] F. Vignola, P. Harlan, R. Perez, M. Kiniecik, Analysis of satellite derived beam and global solar radiation data, Sol. Energy 81 (2007) 768–772.
[23] J. Alonso, F.J. Batlles, Short and medium-term cloudiness forecasting using remote sensing techniques and sky camera imagery, Energy 73 (2014) 890–897.